Electronic Supplementary Material (ESI) for Journal of Materials Chemistry A.
This journal is © The Royal Society of Chemistry 2016

Electronic Supplementary Material (ESI) for Journal of Materials Chemistry A.
This journal is © The Royal Society of Chemistry 2016.

Electronic Supporting Information

Integrating photosystem II into porous TiO_2 nanotube network toward highly-efficient photo-bioelectrochemical cells

Jiao Li,[ab] Xiyun Feng,[ac] Jinbo Fei,[ac] Peng Cai,[ac] Jianguo Huang*[b] and Junbai Li*[ac]

[a]*Beijing National Laboratory for Molecular Sciences (BNLMS), CAS Key Lab of Colloid, Interface and Chemical Thermodynamics, Institute of Chemistry, Chinese Academy of Sciences, Beijing 100190, China.*
E-mail: jbli@iccas.ac.cn; Fax: +86 10 82612629; Tel: +86 10 82614087
[b]*Department of Chemistry, Zhejiang University, Hangzhou, Zhejiang 310027, China.*
E-mail: jghuang@zju.edu.cn; Fax: +86 571 87951202; Tel: +86 571 87951202
[c]*University of Chinese Academy of Sciences, Beijing 100049, China.*

Incident Photon-to-current Conversion Efficiency Measurements

The incident photon-to-current conversion efficiencies (IPCE) of the PSII/$(TiO_2)_5$-NTs-modified ITO electrode were calculated utilizing the following equation:

$$\mathrm{IPCE} = jhc/eP\lambda$$

where h is Planck's constant, c is the vacuum velocity of light, λ is the central wavelength of the incident light and e is the charge of an electron. The generated photocurrent density (j) and the light power density (P) were recorded in the corresponding photoelectrochemical measurement. It was supposed that all incident photons were absorbed by the hybrid photoanode.

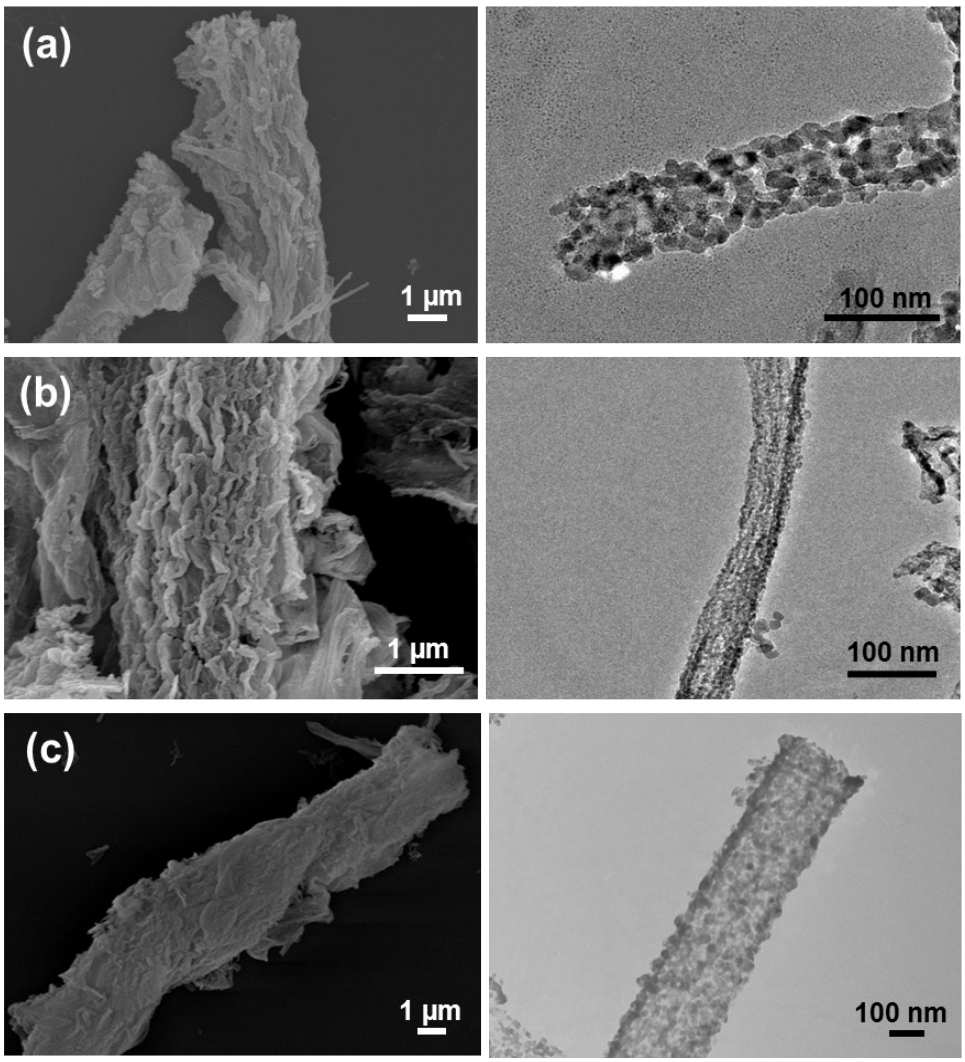

Fig. S1 Left column shows overview FE-SEM images of $(TiO_2)_5$-NTs (a), $(TiO_2)_{10}$-NTs (b) and $(TiO_2)_{20}$-NTs (c). Right column displays TEM images of the corresponding individual titania nanotube.

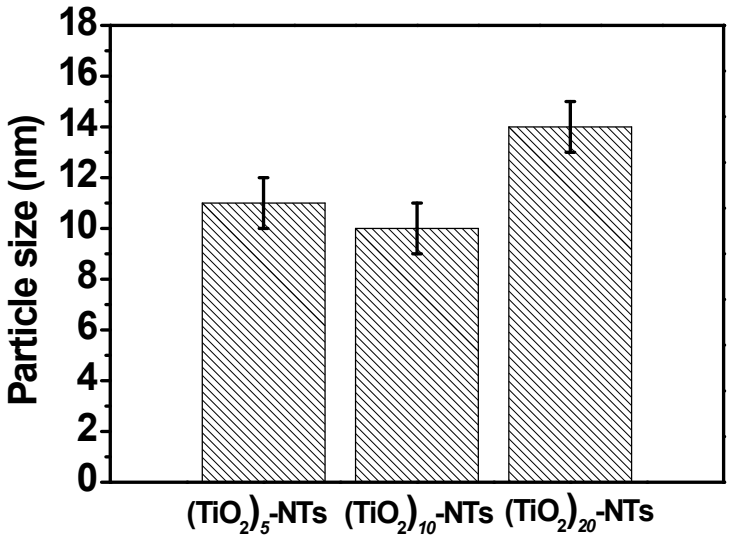

Fig. S2 Average sizes of the nanoparticles in $(TiO_2)_5$-NTs, $(TiO_2)_{10}$-NTs and $(TiO_2)_{20}$-NTs. Error bars represent standard error of the mean, for N = 5 independent experiments, and fifty nanoparticles were taken in each experiment.

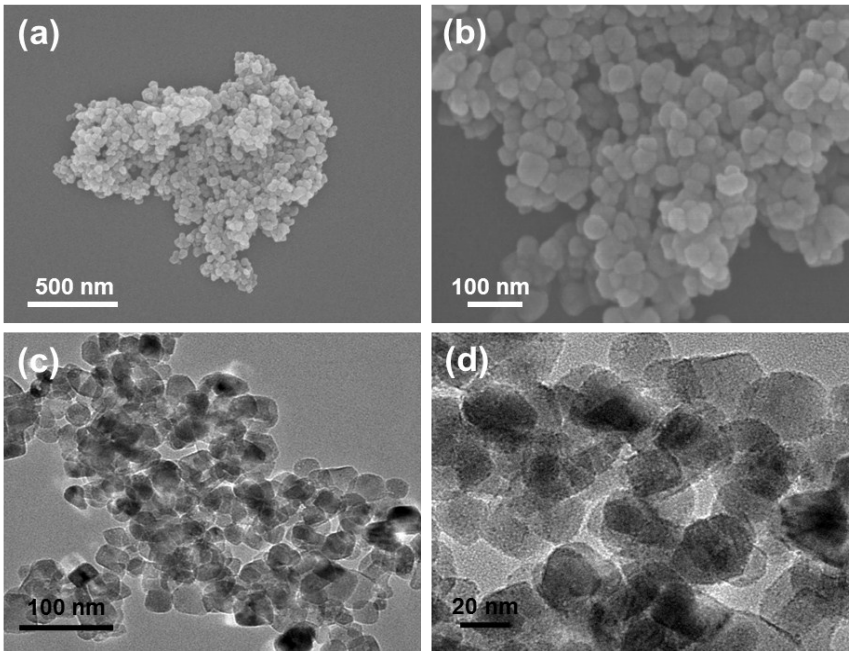

Fig. S3 Overview (a) and enlarged (b) FE-SEM images of the commercial titania nanopowder (TiO_2(C)). Overview (c) and enlarged (d) TEM images of the commercial titania nanopowder (TiO_2(C)).

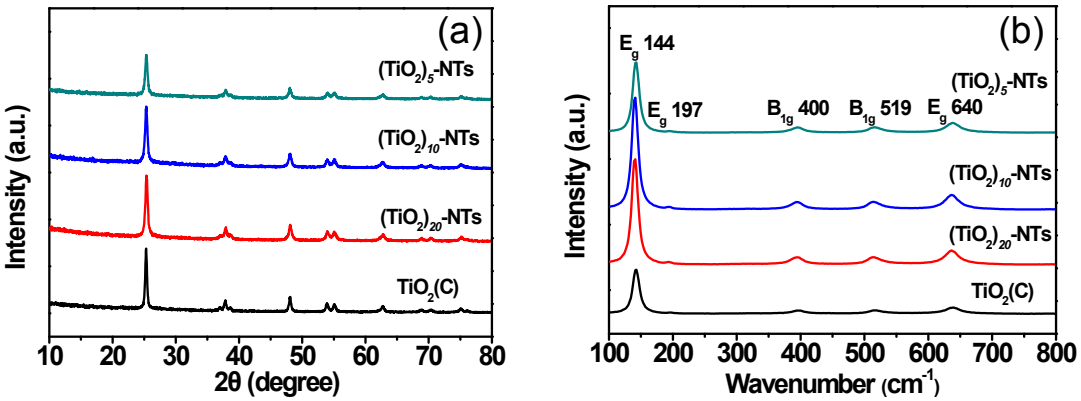

Fig. S4 (a) XRD patterns and (b) Raman spectra of $(TiO_2)_5$-NTs, $(TiO_2)_{10}$-NTs, $(TiO_2)_{20}$-NTs and TiO_2(C).

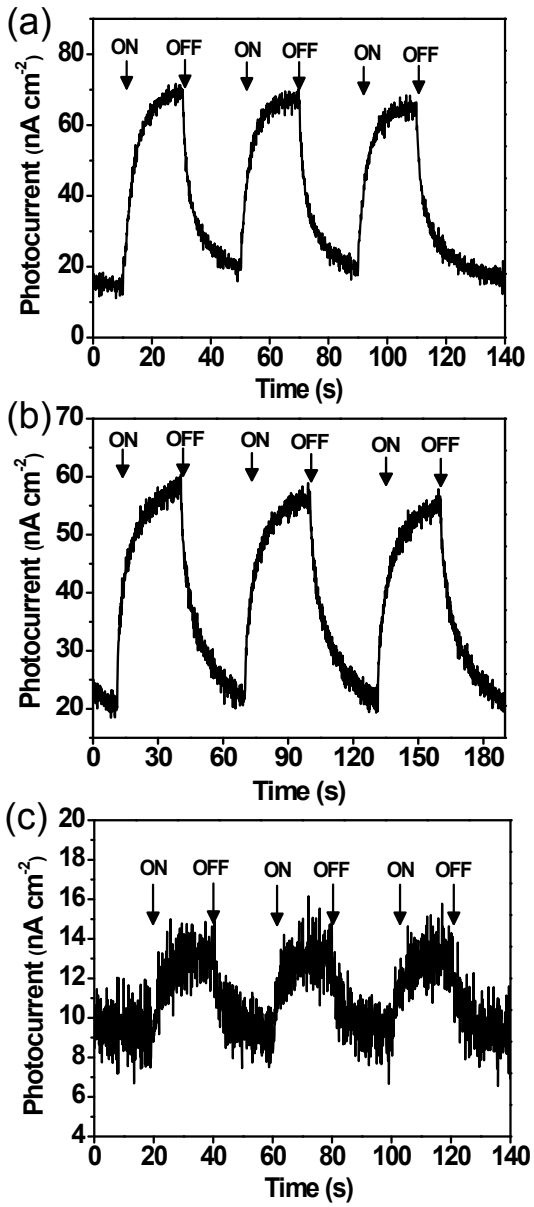

Fig. S5 DET photocurrent responses of (a) PSII/$(TiO_2)_{10}$-NTs, (b) PSII/$(TiO_2)_{20}$-NTs and (c) PSII/TiO_2(C)-modified ITO electrodes to repetitive illumination by red light ($550 < \lambda < 800$ nm, 10 mW cm^{-2}) and darkness cycles. A bias potential of +0.25 V *vs.* SCE was applied at 25 ºC.

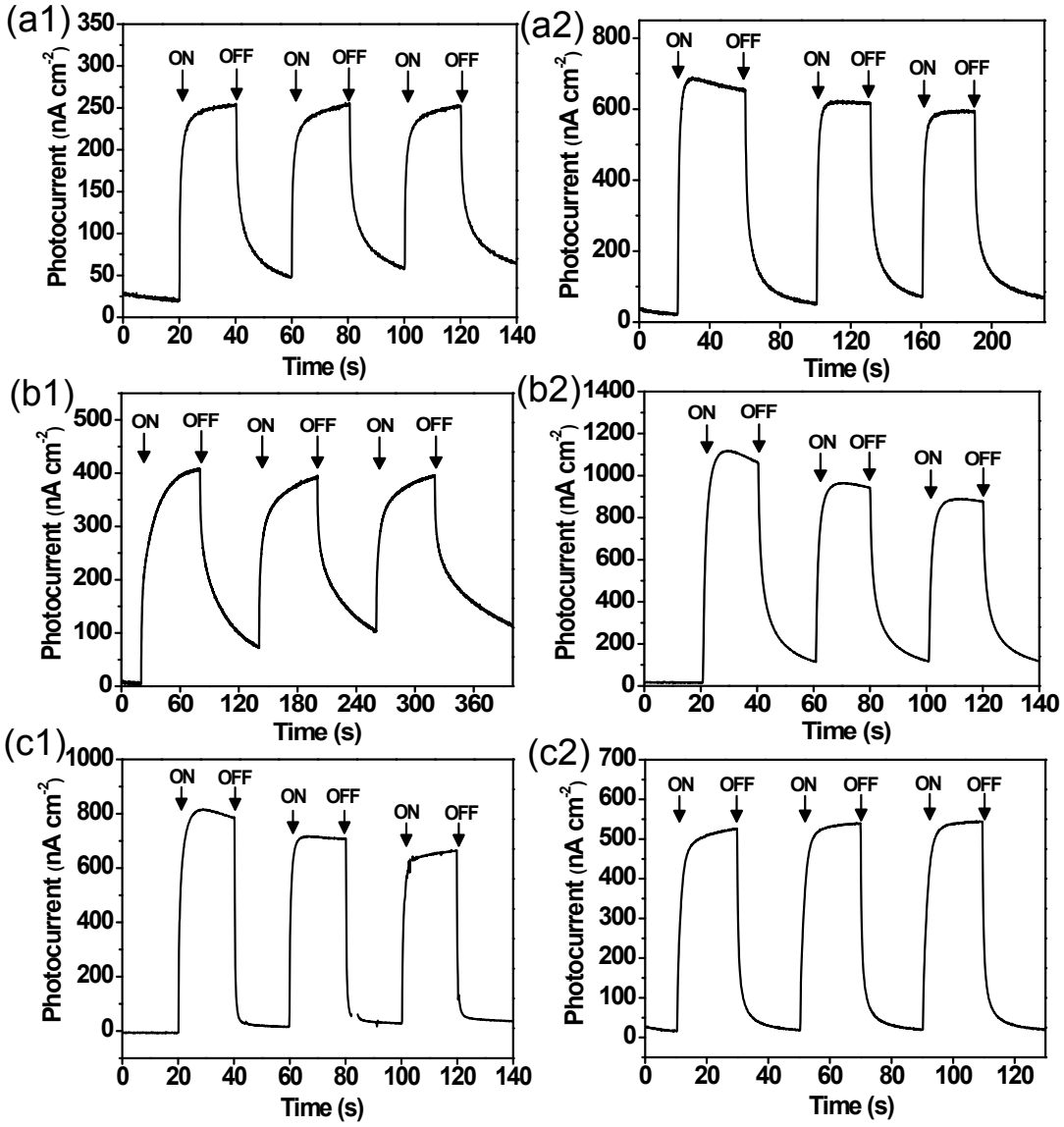

Fig. S6 DET photocurrent responses of bare titania (a1) $(TiO_2)_{10}$-NTs, (b1) $(TiO_2)_{20}$-NTs and (c1) TiO_2(C)-modified ITO electrodes to repetitive illumination by white light and darkness cycles. DET photocurrent responses of (a2) PSII/$(TiO_2)_{10}$-NTs, (b2) PSII/$(TiO_2)_{20}$-NTs and (c2) PSII/TiO_2(C)-modified ITO electrodes to repetitive illumination by white light and darkness cycles. A bias potential of +0.25 V *vs.* SCE was applied at 25 ºC.

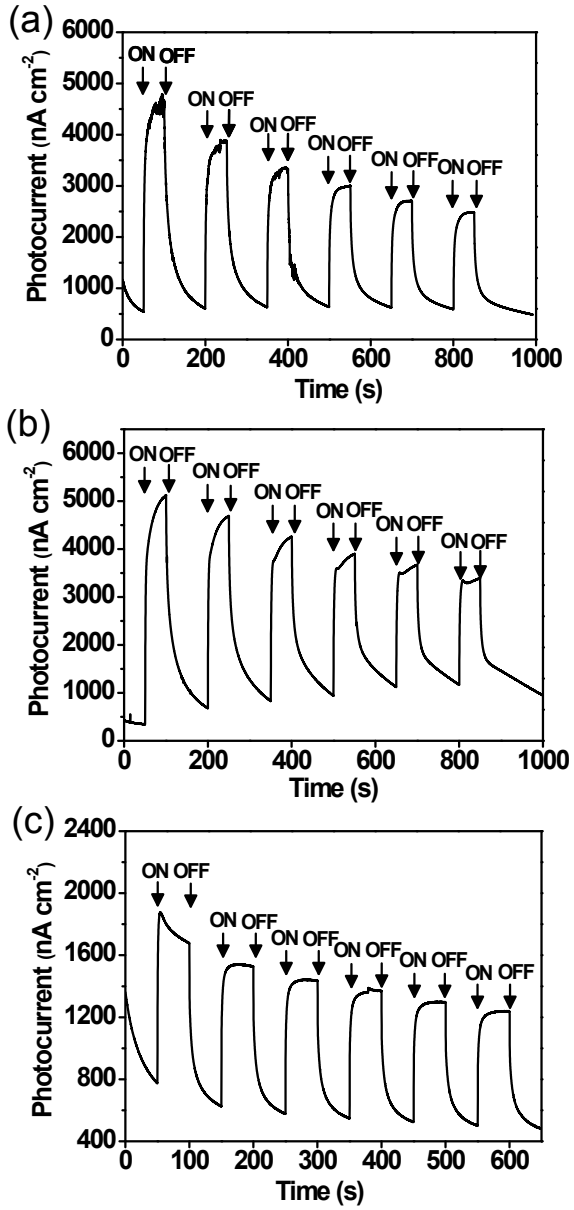

Fig. S7 MET photocurrent responses of (a) PSII/$(TiO_2)_{10}$-NTs, (b) PSII/$(TiO_2)_{20}$-NTs and (c) PSII/TiO_2(C)-modified ITO electrodes with 1 mM DCBQ in the electrolyte to repetitive illumination by red light ($550 < \lambda < 800$ nm, 10 mW cm^{-2}) and darkness cycles. A bias potential of +0.25 V *vs.* SCE was applied at 25 ºC.

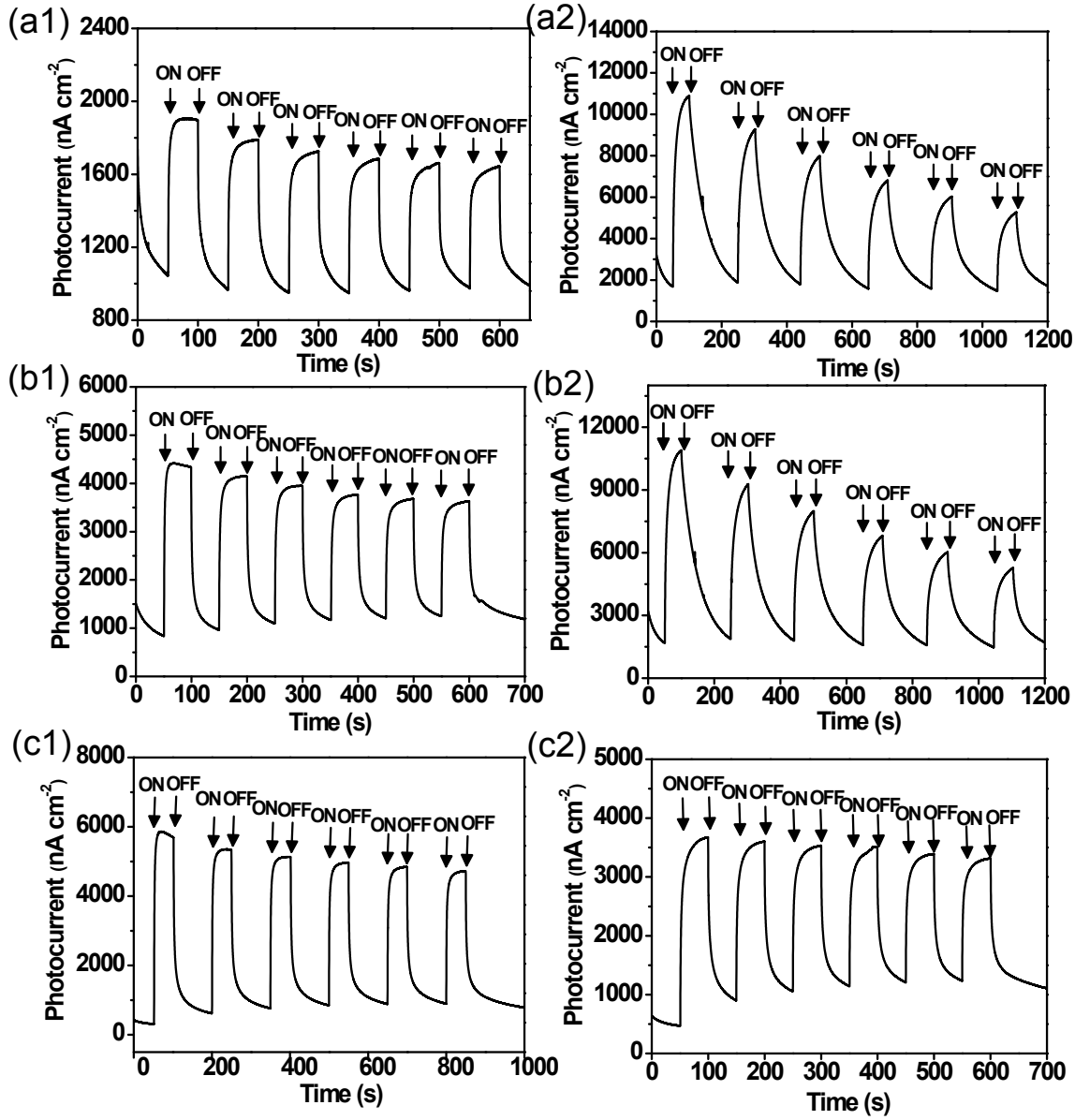

Fig. S8 MET photocurrent responses of bare titania (a1) $(TiO_2)_{10}$-NTs, (b1) $(TiO_2)_{20}$-NTs and (c1) TiO_2(C)-modified ITO electrodes with 1 mM DCBQ in the electrolyte to repetitive illumination by white light and darkness cycles. MET photocurrent responses of (a2) PSII/$(TiO_2)_{10}$-NTs, (b2) PSII/$(TiO_2)_{20}$-NTs and (c2) PSII/TiO_2(C)-modified ITO electrodes with 1 mM DCBQ in the electrolyte to repetitive illumination by white light and darkness cycles. A bias potential of +0.25 V *vs.* SCE was applied at 25 ºC.

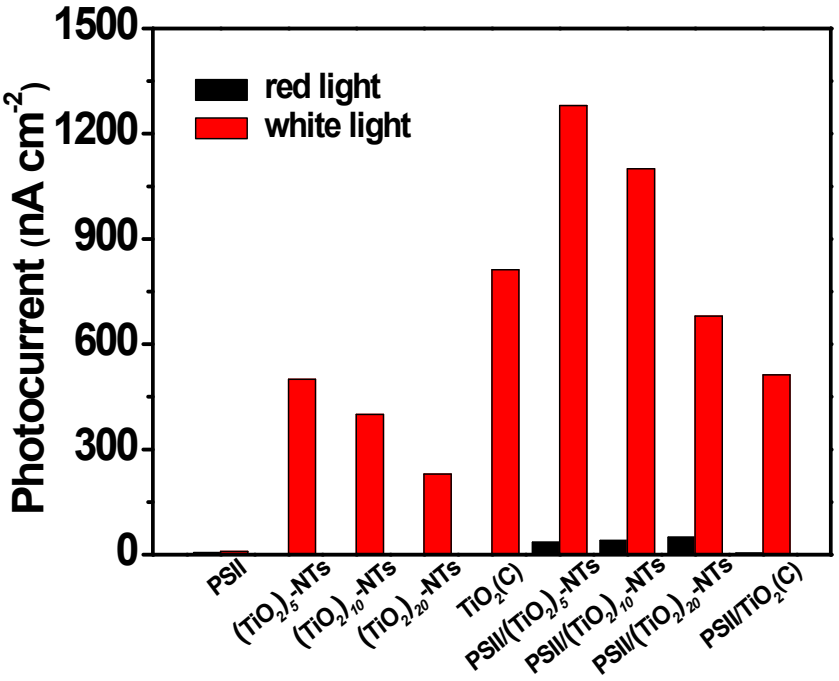

Fig. S9 Comparisons of DET photocurrent responses of PSII, $(TiO_2)_5$-NTs, $(TiO_2)_{10}$-NTs, $(TiO_2)_{20}$-NTs, TiO_2(C), PSII/$(TiO_2)_5$-NTs, PSII/$(TiO_2)_{10}$-NTs, PSII/$(TiO_2)_{20}$-NTs and PSII/TiO_2(C)-modified ITO electrodes under red light and white light irradiations.

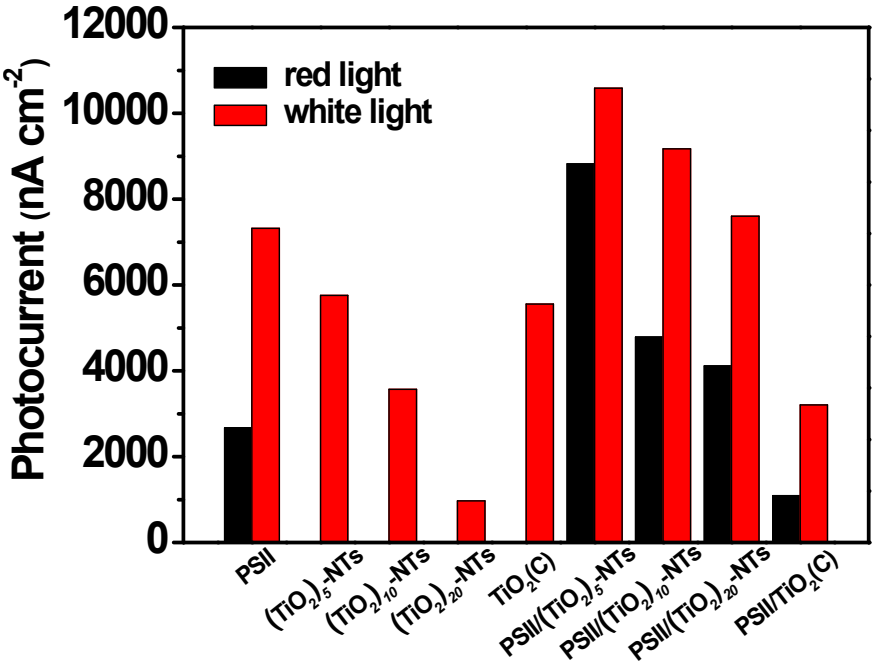

Fig. S10 Comparisons of MET photocurrent responses of PSII, $(TiO_2)_5$-NTs, $(TiO_2)_{10}$-NTs, $(TiO_2)_{20}$-NTs, TiO_2(C), PSII/$(TiO_2)_5$-NTs, PSII/$(TiO_2)_{10}$-NTs, PSII/$(TiO_2)_{20}$-NTs and PSII/TiO_2(C)-modified ITO electrodes under red light and white light irradiations.

Table S1 Summary of photoelectrochemical performance of PSII PF-PEC cells.

Reference	Electrode	origin	Light (nm)	Bias potential (V *vs.* SCE)	*j* (μA cm^{-2}) DET	*j* (μA cm^{-2}) MET	Half-life time (min)	IPCE (%)
23	PSII/Ni-NTA/Au	*T. elongatus*	675	0.26		14[a]	18	
24	PSII/Ni-NTA/Au	*T. vulcanus*	680	0.16	0.13			
	PSII/Ni-NTA/Au (nanoparticles)	*T. vulcanus*	680	0.16	2.4			
26	PSII/pMBQ/Au	*M. laminosus*	> 400	0.15		2.7		1.0
27	PSII/Os redox polymer/Au	*T. elongatus*	675	0.26		45	~ 55	
28	PSII/PBV^{2+}/PSII/PBV^{2+}	*M. laminosus*	675	-0.04	0.5			~ 0.3
31	PSII/mesoITO	*T. elongatus*	635	0.26	1.6		< 5	
						12[b]		0.3[b]
						22[a]		
32	PSII/$C_2CO_2^-$/mesoITO (electrostatic)	*T. elongates*	679	0.26	0.28		< 5	0.005
						1.4[a]		0.03[a]
	PSII/$C_2CO_2^-$/mesoITO (covalent)	*T. elongates*	679	0.26	0.43		~ 12	0.01
						4.5[a]		0.10[a]
This work	PSII/$(TiO_2)_5$-NTs/ITO	*spinach*	550 ~ 800	0.25	0.035			~ 0.0006
						8.8[a]		~ 0.16[a]
			White light		1.3		~ 14	~ 0.02
						10.6[a]		~ 0.19[a]

[a] Mediated electron transfer using DCBQ. [b] Mediated electron transfer using potassium 1,4-naphthoquinone-2-sulfonate (NQS).